2016

Elasto-Plastic Transient Dynamic Response of Tubular Section Steel Cantilever Beam Under Impact Loading

AliAl Aloosi
Old Dominion University

Zia Razzaq
Old Dominion University, zrazzaq@odu.edu

Original Publication Citation

Aloosi, A., & Razzaq, Z. (2016). Elasto-plastic transient dynamic response of tubular section steel cantilever beam under impact loading. *Global Journals of Research in Engineering*, *16*(E5), 7-15. https://engineeringresearch.org/index.php/GJRE/article/view/1524

Global Journal of Researches in Engineering: E
Civil And Structural Engineering
Volume 16 Issue 5 Version 1.0 Year 2016
Type: Double Blind Peer Reviewed International Research Journal
Publisher: Global Journals Inc. (USA)
Online ISSN: 2249-4596 & Print ISSN: 0975-5861

Elasto-Plastic Transient Dynamic Response of Tubular Section Steel Cantilever Beam under Impact Loading

By AliAl Aloosi & Zia Razzaq
Old Dominion University

Abstract- This paper presents the outcome of an experimental and theoretical investigation into the load-carrying capacity of Fiber Reinforced Polymer (FRP) I-section beams subjected to four-point loading. The overall lateral-torsional buckling, web and flange local buckling as well as material rupture load estimates are also made using the American Society of Civil Engineers' Load and Resistance Factor Design (ASCE-LRFD) Pre-Standard for FRP Structures. Lateral-torsional buckling failure mode is found to govern for each of the beams studied. The study also revealed that the height of applied loads relative to the shear center has a very significant influence on lateral-torsional buckling load of a beam thus making ASCE-LRFD buckling load estimates over-conservative in a vareity of cases.

Keywords: impact, dynamic, elasto-plastic, flexural dynamic equilibrium.

GJRE-E Classification: FOR Code: 090506

Strictly as per the compliance and regulations of :

Elasto-Plastic Transient Dynamic Response of Tubular Section Steel Cantilever Beam under Impact Loading

AliAl Aloosi [α] & Zia Razzaq [σ]

Abstract- This paper presents the outcome of a theoretical and experimental study of the dynamic elasto-plastic behavior of a steel cantilever beam. An apparatus is constructed and used for conducting a series of experiments by applying a vertical impact load on the cantilever. A mathematical prediction model based on a partial differential equation of flexural dynamic equilibrium is formulated including new nonlinear terms to account for the elasto-plastic behavior of a steel cantilever beam. The experimental results are found to be in good agreement with the predicted behavior.

Keywords: impact, dynamic, elasto-plastic, flexural dynamic equilibrium.

I. Introduction

Razzaq et al. [1] conducted a theoretical and experimental study of slender tubular columns with partial rotational end restraints in the presence of initial imperfections. New explicit formulas and finite-difference formulation were derived for predicting the elastic buckling load and predicting the natural frequency. Jones [2] studied the behavior of fully clamped beams when struck at the mid-span by a rigid mass and compared it with the corresponding exact theoretical predictions of dynamic rigid-plastic analyses. Wen et al. [3] proposed a quasi-static procedure based on the principle of virtual work for estimating the dynamic plastic response and failure of clamped metal beams subjected to a low velocity impact at any point on the span by a heavy mass. The paper by Zeinoddini et al [4] described experimental studies in which axially pre-loaded tubes were examined under lateral dynamic impact loads. The tubes were impacted by a dropped object with a velocity of about 7 meter/sec at their mid-span.

The current paper presents the outcome of an experimental and theoretical study of a partially end-restrained cantilever beam under impact loading. New terms are added to the governing dynamic equilibrium equation for the problem to account for elasto-plastic effects when transient dynamic response of the cantilever needs to be predicted.

Author α: Research Assistant, Department of Civil and Environmental Engineering, Old Dominion University, 115 Kaufman Hall, Norfolk, Virginia. e-mail: aalal001@odu.edu

Author σ: University Professor, Department of Civil and Environmental Engineering, Old Dominion University, 135 Kaufman Hall, Norfolk, Virginia. e-mail: zrazzaq@odu.edu

Numerical results are obtained using an iterative finite-difference procedure. The iterative solution process also involves a materially nonlinear tangent stiffness method to deal with cross-sectional plastification as a funcation of time.

II. Experimental Study

Figure 1 shows schematic of a cantilever beam QB subjected to a forcing function F(t) generated by a freely falling impact load. For the beam, the origin of the longitudinal ordinate z is at Q. At end B, the cantilever beam is attached to a rotationally flexible elastic support simulated as a rotational spring having a rotational spring constant valule of $k_B=6x10^6$ kip-in/rad. The cantilever beam QBhas a length L of 33 in. and a 2x2x0.125 in. hollow square cross section. The test set-up is shown in Figure 2.

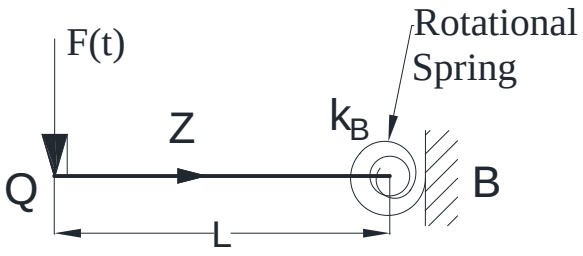

Figure 1: Analysis model of the cantilever

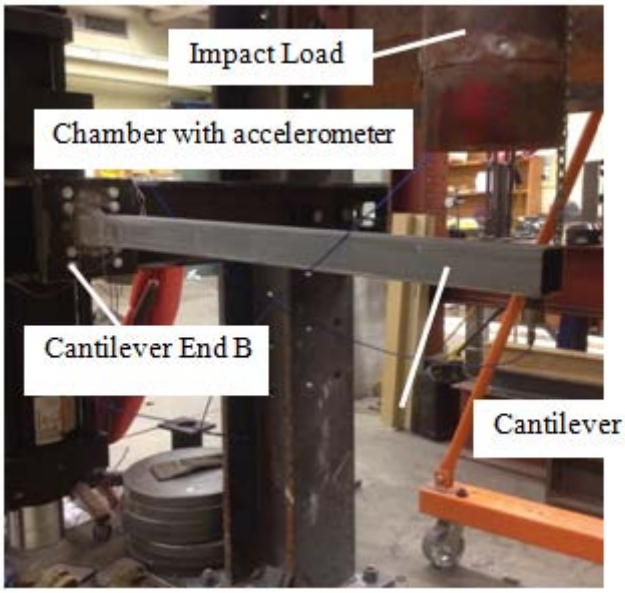

Figure 2: Test setup

The impact tests were performed using three different impactors numbered 1, 2, and 3 weighing 60 lb., 140 lb., and 400 lb., respectively. Each impactor had an accelerometer inside a steel chamber attached at the impactor bottom end to record acceleration-time relationship which was curve-fitted using a quadratic function of time t. The relationships marked C1-1, C1-2, and C1-3 shown in Figure 3 correspond to Impactors 1, 2, and 3 each dropped onto the cantilever beam with a gap of one inch between the cantilever beam's top surface and the bottom face of the steel chamber. In the same figure, the relationship marked C1-4 is for Impactor 3 dropped with a gap of two inches. The forcing function F(t) is generated by multiplying the ordinate of Figure 3 by mg, where m is the impactor mass and g is 32.2 ft./sec^2.The forcing functions for Impactors 1, 2, and 3 when dropped from 1 inch height are as follow:

$$F_1(t) = (-6338.8\, t^2 + 418.56\, t - 3.0877)\ mg \quad \text{for} \quad 0.008 \le t \le 0.057 \qquad (1)$$

$$F_2(t) = (-2506.8\, t^2 + 241.92\, t - 2.8519)\ mg \quad \text{for} \quad 0.008 \le t \le 0.083 \qquad (2)$$

$$F_3(t) = (-628.55\, t^2 + 91.886\, t - 1.4533)\ mg \quad \text{for} \quad 0.008 \le t \le 0.129 \qquad (3)$$

The forcing function for Impactor 3 when dropped from 2 inches height is as follows:

$$F_4(t) = (-804.63\, t^2 + 111.12\, t - 1.4058)\ mg \quad \text{for} \quad 0.008 \le t \le 0.125 \qquad (4)$$

The lower limit represents the time when the impactor hits the cantilever beam tip while the upper limit represents the time when the impactor is deatached from the beam.

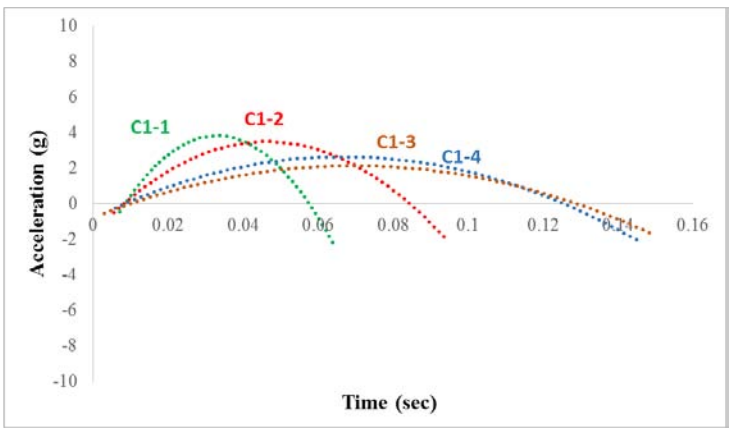

Figure 3: Curve-fitted acceleration-time relations

Three strain gauges were installed on the cantilever beam to measure strain-time histories. The strain gauges, designated as SG1, SG2, and SG3, were installed on the cantilever beam at three locations at a distance of one inch from end B as shown in Figure 4.

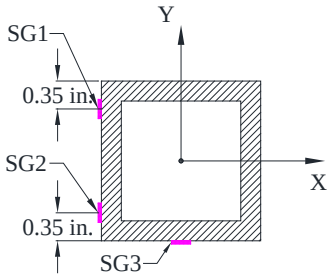

Figure 4: Location of strain gauges at section B

III. Theoretical Study

The elastic dynamic flexural equilibrium equation for a beam without damping is given in the literature [5] as follows:

$$EI\frac{\partial^4 v}{\partial z^4} + m\frac{\partial^2 v}{\partial t^2} = F(t) \quad (5)$$

in which $EI$is the elastic flexural rigidity, $v$is the beam deflection, $m$is the beam mass per unit length, $z$is the horizontal distance along the member, $t$is the time, and F(t)is aforcing function. In the inelastic range, EI changes with the applied load. Therefore, the inelastic partial differential equation of motion can be expressed as:

$$\frac{\partial^2}{\partial z^2}\left(B_e\frac{\partial^2 v}{\partial z^2}\right) + m\frac{\partial^2 v}{\partial t^2} = F(t) \quad (6)$$

where B_e is the elasto-plastic flexural rigidity.In this equation, damping is not included since it is negligible due to the predominant influence of impact loading on the beam response for the duration of the impact. For a given time t, $B_e$is a function of z, thus Equation 6 becomes:

$$B_e\frac{\partial^4 v}{\partial z^4} + 2\frac{\partial^3}{\partial z^3}\left(\frac{\partial B_e}{\partial z}\right) + \frac{\partial^2 v}{\partial z^2}\left(\frac{\partial^2 B_e}{\partial z^2}\right) + m\frac{\partial^2 v}{\partial t^2} = F(t) \quad (7)$$

To obtain the numerical results presented in this paper, the first and second partial derivatives of$B_e$appearing in Equation 7 were iteratively generated with Lagrangian polynomials along the z axis.

a) Boundary Conditions

At Q in Figure 1, the bending moment is zero, thus:

$$m_Q = \frac{\partial^2 v}{\partial z^2}(0,t) = 0 \quad (8a)$$

The shear force at Q can be expresses as:

$$V_Q = \frac{\partial^3 v}{\partial z^3}(0,t) = -F(t) \quad (8b)$$

At end B, the cantilever beam has no vertical movement:

$$v_{(L,t)} = v_B = 0 \quad (8c)$$

The elastic moment-rotation relationship of the rotational spring at B is expressed as:

$$m_B = k_B\theta_B \quad (8d)$$

Where k_B is the stiffness of the rotational spring at end B, and $\theta_B$is the rotation of the cantileverbeam at the same location. Since$\theta_B$is the first derivative of the deflection at end B, thus:

$$\theta_B = -v'(L) \quad (8e)$$

The minus sign in this equation is consistent with downward deflections taken as positive in the derivation of Equation 7. The boundary conditions presented above are used in the elasto-plastic dynamic analysis of the cantilever beam.

b) Initial Conditions

The initial conditions for the problem are:

$$v(z,0) = 0 \quad (9a)$$

$$\frac{\partial v}{\partial t}(z,0) = 0 \quad (9b)$$

The initial condition given by Equation 9a states that at time t equal zero, the deflection is zero. Equation 9b states that the initial velocity is zero.

c) Finite-Difference Solution

Central finite-difference expressions [6] were used to solve Equation 7 with boundary and intial conditions presented in Sections 3.1 and 3.2. A total of N panels were used for the cantilever beam over the interval (0, L) involving nodes i = 1, 2, 3, …. (N+1). The finite-difference scheme also results in 'phantom points' outside of the interval (0,L) and are accounted-for in the solution algorithm. Using second order finite-difference expressions, Equation 7 can be written as:

$$\frac{B_e}{h^4}\left(v_{i-2,j} - 4v_{i-1,j} + 6v_{i,j} - 4v_{i+1,j} + v_{i+2,j}\right)$$
$$+\frac{2}{h^3}\left(-v_{i-2,j} + 2v_{i-1,j} - 2v_{i+1,j} + v_{i+2,j}\right)\left(\frac{\partial B_e}{\partial z}\right)$$
$$+\frac{1}{h^2}\left(v_{i-1,j} - 2v_{i,j} + v_{i+1,j}\right)\left(\frac{\partial^2 B_e}{\partial z^2}\right) + \frac{m}{(\Delta t)^2}\left(v_{i,j-1} - 2v_{i,j} + v_{i,j+1}\right) = F(t) \quad (10)$$

in which, h is the panel length along the z-axis of the sub-assemblage, and Δt is the time interval. The subscript i refers to the ith nodal point over the domain $0 < x < L$, and the subscript j refers to the number of time increments such that the time at j is given by the following equation:

$t_j = j(\Delta t)$, for each $j = 0, 1, 2, 3, \ldots$

Similarly, the boundary conditions 8a, 8b, 8c, and 8d can be expressed in finite-difference form as follows:

$$\left(\frac{1}{h^2}\right)\left(v_{0,j} - 2v_{1,j} + v_{2,j}\right) = 0 \quad (11a)$$

$$\left(\frac{1}{2h^3}\right)\left(-v_{-1,j} + 2v_{0,j} - 2v_{2,j} + v_{3,j}\right) = -F(t) \quad (11b)$$

$$v_{N+1,j} = 0 \quad (11c)$$

$$\left(\frac{B_e}{h} + \left(\frac{K_B}{2}\right)\right)\left(v_{N+2,j}\right) - \left(\frac{2B_e}{h}\right)\left(v_{N+1,j}\right) - \left(\frac{-B_e}{h} + KB2vN,j=0\right) \quad (11d)$$

Applying Equation 10 at i=1, 2, 3…, N, and invoking conditions 11a, 11b, 11c, and 11d leads to the following matrix equation:

$$\{v_{i,j+1}\} = C_1[\aleph]\{v_{i,j}\} + C_2\{v_{i,j-1}\} - C_1\{F(t)\} \quad (12)$$

in which

$$C_1 = -\frac{1}{(b_3)} \quad (13a)$$

$$C_2 = b_3 C_1 \quad (13b)$$

$$b_3 = \frac{m}{(\Delta t)^2} \quad (13c)$$

The $[\aleph]$coefficient matrix is symmetric and of the order NxN.

A finite-difference iterative algorithm was developed for the nonlinear dynamic analysis of the cantilever beam. The deflections along the cantilever beam were found for the first time increment using the elastic formula. To avoid having a negative time interval due to the use of central finite-difference, a start-up equation [1] was used to initialize the process. Initial nodal deflections were found using Equation 10.An iterative tangent stiffness procedure was utilized to compute the curvatures due to the applied moments which satisfied cross-sectional equilibrium. Next, the elasto-plastic cross-sectional properties were calculated using the computed curvatures, and Revised deflections were found using the updated cross-sectional properties. The revised deflections were compared with the intial deflections for the same time increment. If the difference was found to be larger than a specified tolerance value, another iteration was performed for that time increment. If the difference was found to be smaller than a tolerance value, the procedure was continued to the next time increment with the corresponding new value of the forcing forcing function. This solution procedure was used to generate the theoretical strain-time curves shown in Figures 5 through 12.

d) Cantilever Behavior under Impact Loading

Table 1 compares the maximum experimental and theoretical moments at section B of the cantileverbeam for Tests C1-1, C1-2, C1-3, and C1-4. For Test C1-1, Impactor 1 was dropped from one inch above end Q of the cantilever beam. Figures 5 and 6 show theoretical and experimental strain-time curves for SG1 and SG2, respectively. Both figures show the same trending, and the peak values agreed well. The ratios between the tested to the predicted strain results ranged from 0.99 to 1.17.

Table 1: Comparison between theoretical and experimental maximum moments at B for the cantilever beam impact tests

Test	Theoretical	Experimental
	Max. Moment at B (kip-in.)	Max. Moment at B (kip-in.)
C1-1	9.4	10.8
C1-2	17.8	20.3
C1-3	37.7	38.1
C1-4	39.8	39.5

Table 2 shows the experimental and the theoretical strains, and their comparison. For this test, the experimental maximum moment at section B was 10.8 kip-in. and the theoretical value was 9.4 kip-in. The difference between the theoretical and the experimental results was 15%. The experimental and the theoretical moment values were in good agreement and they were in the elastic range.

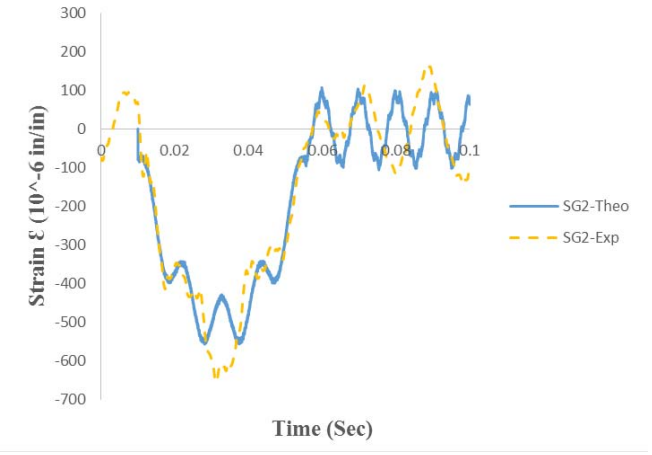

Figure 5: Comparison of theoretical and experimental strain-time relations of SG1for test C1-1

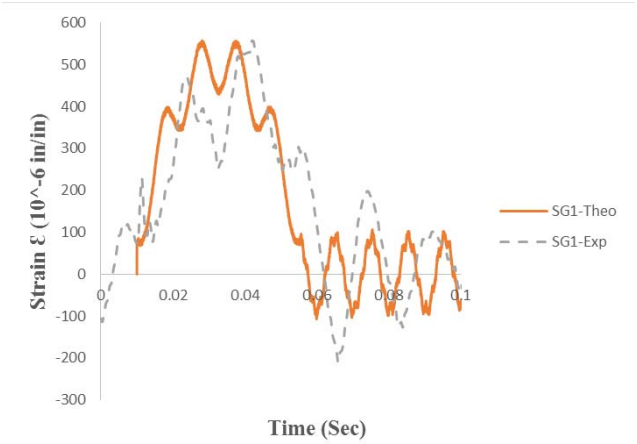

Figure 6: Comparison of theoretical and experimental strain-time relations of SG2 for test C1-1

Table 2: Experimental and theoretical strains for test C1-1

Strain gauge	Experimental strain (in./in.)	Theoretical Strain (in./in.)	Experimental / Theoretical
SG1	0.000557	0.000557	0.999477
SG2	-0.00065	-0.00056	1.17443

For Test C1-2, Impactor 2 was dropped from one inch above end Q of the cantilever beam. Figures 7 and 8 show the theoretical and the experimental strain-time curves for SG1 and SG2, respectively. Table 3 shows the experimental and the theoretical strains and, their comparison. The ratios between the tested to the predicted strain results ranged from 0.93 to 1.01. For this test, the experimental maximum moment at section B was 20.3 kip-in and the theoretical value was 17.8 kip-in. The difference between the theoretical and the experimental results was 14%. A good agreement was reached between the tested and the predicted results. Results from this test were in the elastic range.

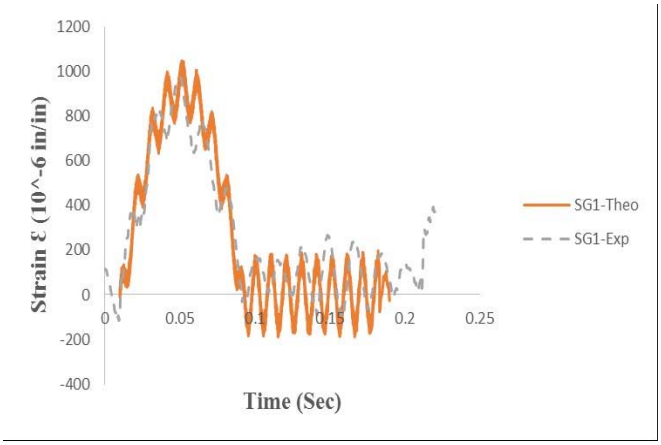

Figure 7: Comparison of theoretical and experimental strain-time relations of SG1for test C1-2

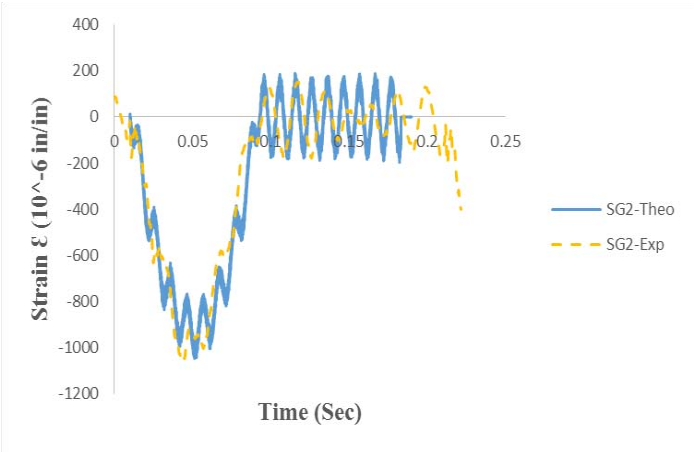

Figure 8: Comparison of theoretical and experimental strain-time relations of SG2 for test C1-2

Table 3: Experimental and theoretical strains for test C1-2

Strain gauge	Experimental strain(in./in.)	Theoretical strain(in./in.)	Experimental / Theoretical
SG1	0.000971	0.001046	0.927865
SG2	-0.00106	-0.00105	1.011955

For Test C1-3, Impactor 3 was dropped from one inch above end Q of the cantilever. Figures 9 and 10 show the theoretical and the experimental strain-time curves for SG1 and SG2, respectively. Table 4 shows the experimental and the theoretical strains and, their comparison. The ratios between the tested to the predicted strain results ranged from 0.89 to 0.86, which are considered to be reasonable results. There was an overall good agreement in the shape of all the load-strain curves. For this test, the experimental maximum moment at section B was 38.1 kip-in and the theoretical value was 37.7 kip-in. The difference between the theoretical and the experimental results was 2%. Both the experimental and the theoretical curves were very similar and their peak values were very close. This test caused partial plastification on the cantilever beam.

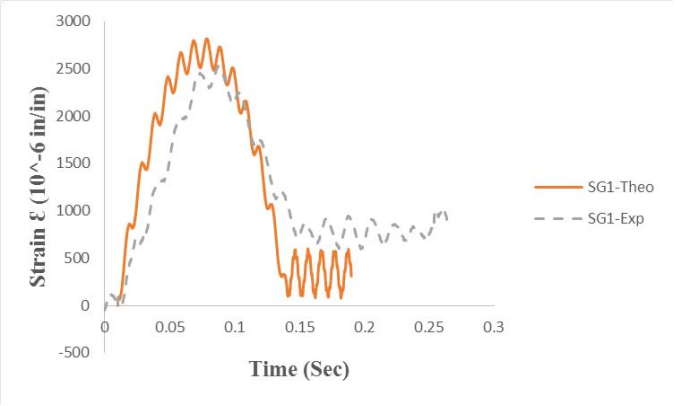

Figure 9: Comparison of theoretical and experimental strain-time relations of SG1for test C1-3

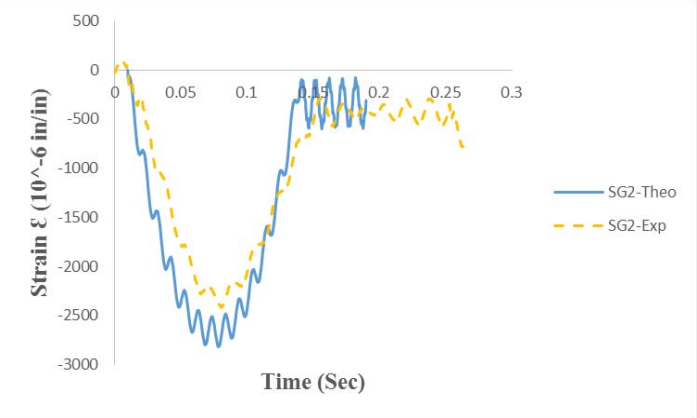

Figure 10: Comparison of theoretical and experimental strain-time relations of SG2 for test C1-3

Table 4: Experimental and theoretical strains for test C1-3

Strain gauge	Experimental strain (in./in.)	Theoretical strain (in./in.)	Experimental / Theoretical
SG1	0.002531	0.002817	0.898389
SG2	-0.00242	-0.00282	0.859344

For Test C1-4, Impactor 3 was dropped from two inches above end Q of the cantilever. Figures 11 and 12 show the theoretical and the experimental strain-time curves for SG1 and SG2, respectively. Table 5 shows the experimental and theoretical strains, and their comparison. The ratios between the tested to the predicted strain results ranged from 1.01 to 1.06. For this test, the experimental maximum moment at section B was 39.5 kip-in and the theoretical value was 39.2 kip-in. Both the theoretical and the experimental results showed the formation of a plastic hinge at section B. It can be seen that there was good agreement between the predicted and the experimental values for the strains and the moments.

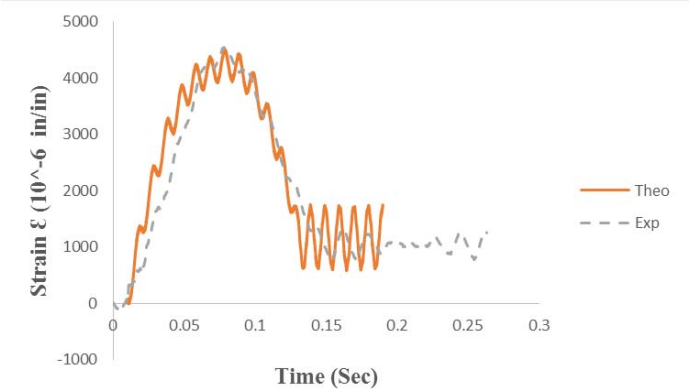

Figure 11: Comparison of theoretical and experimental strain-time relations of SG1for test C1-4

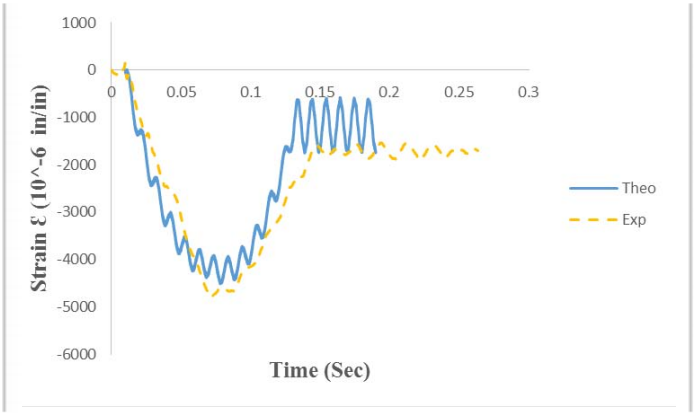

Figure 12: Comparison of theoretical and experimental strain-time relations of SG2 for test C1-4

Table 5: Experimental and theoretical strains for test C1-4

Strain gauge	Experimental strain (in./in.)	Theoretical strain (in./in.)	Experimental / Theoretical
SG1	0.004545	0.004512	1.007121
SG2	-0.004783	-0.004512	1.05997

IV. Conclusion

A theoretical and experimental study of the dynamic elasto-plastic behavior of a steel cantileverbeam is presented. A mathematical model based on a partial differential equation of inelastic dynamic equilibrium is successfully developed including new terms to account for elasto-plastic behavior of a steel cantilever beam. The iterative finite-difference solution algorithm predicted experimental elasto-plastic behavior of the cantilever beam for various impact forcing functions. It was also found that the weight of the impactor is directly related to the total duration of impact. By comparing the curve-fitted acceleration response generated by different impactors, it was found that the maximum curve-fitted acceleration value is inversely related to the mass of the impactor.

References Références Referencias

1. Razzaq, Zia, R.T. Voland, H.G. Bush and Mikulas, M.M.," Stability, Vibration and Passive Damping of Partially restrained imperfect columns", *NASA Technical Memorandum*, No. 85697, October 1983.
2. Jones, N., "Quasi-static Analysis of Structural Impact Damage," J. Construct. Steel Research, No. 33, pp. 151-177, 1995.

3. Wen, H. M., Reddy, T. Y. and Reid, S. R.," Deformation And Failure Of Clamped Beams Under Low Speed Impact Loading," International Journal of Impact Engineering, Vol. 16, No. 3, pp. 435-454, 1995.
4. Zeinoddini, M., Parkeb, G.A.R. and Harding, J.E.," Axially pre-loaded steel tubes subjected to lateral impacts: an experimental study," International Journal of Impact Engineering, No. 27, pp. 669–690, 2002.
5. Warburton, G.B.," The dynamical Behavior of Structures," Pergamon Press Ltd., 1976.
6. Ketter, Robert L., and Prawel Jr., Sherwood P.," Modern Methods of Engineering Computation," McGraw-Hill Companies, 1969.

Global Journal of Researches in Engineering (E) Volume XVI Issue V Version I Year 2016
16

This page is intentionally left blank